Electronic Supplementary Material (ESI) for Photochemical & Photobiological Sciences.
This journal is © The Royal Society of Chemistry and Owner Societies 2019

Effect of Charge Transfer and Structural Rigidity on Divergent Luminescence Response of a Metal Organic Framework towards Different Metal Ions: Luminescence Lifetime Decay Experiments and DFT Calculations

Prakash Majee,[a] Debal Kanti Singha,[a,b] Sudip Kumar Mondal*[a] and Partha Mahata*[b]

[a]Department of Chemistry, Siksha-Bhavana, Visva-Bharati University, Santiniketan-731235, West Bengal, India. Email: sudip.mondal@visva-bharati.ac.in

[b]Department of Chemistry, Jadavpur University, Jadavpur, Kolkata-700 032, West Bengal, India. Email: parthachem@gmail.com

ELECTRONIC SUPPLEMENTARY INFORMATION

* Corresponding Authors, E-mail: sudip.mondal@visva-bharati.ac.in, parthachem@gmail.com

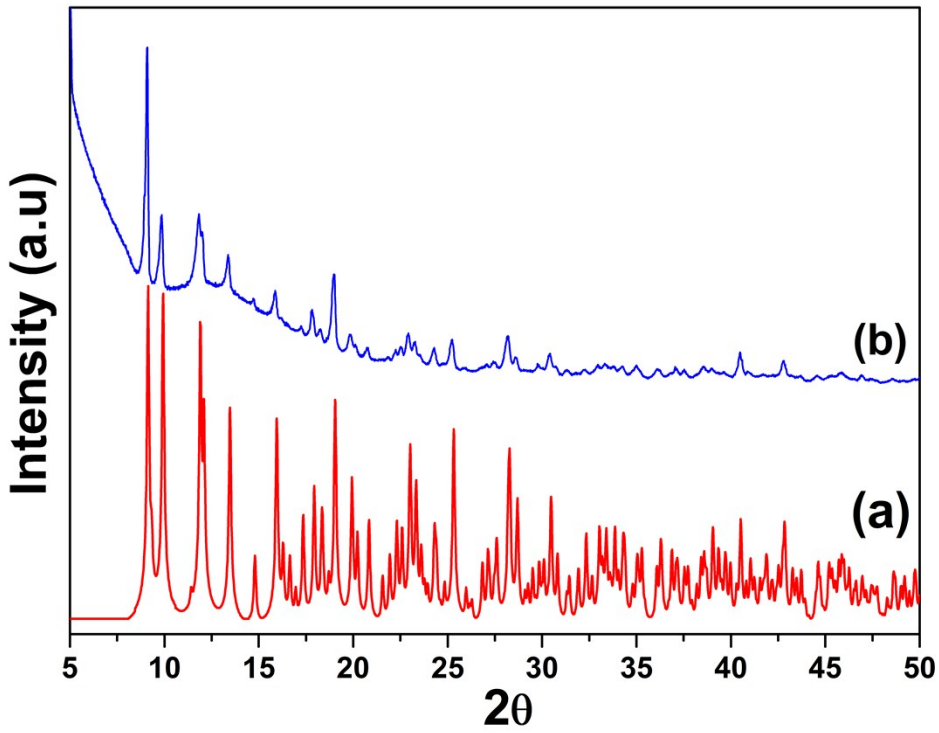

Fig. S1: Powder XRD (CuKα) patterns of $[Cd(C_{12}N_2H_8)(C_7N_1O_4H_3)]$, **1**: (a) simulated from single crystal X-ray data of $[Cd(phen)(2,5\text{-pda})]_\infty$ (Y. Wei, H. Hou,* L. Li, Y. Fan and Y. Zhu, Cryst. Growth Des., 2005, 5(4), 1405-1413) (b) experimental.

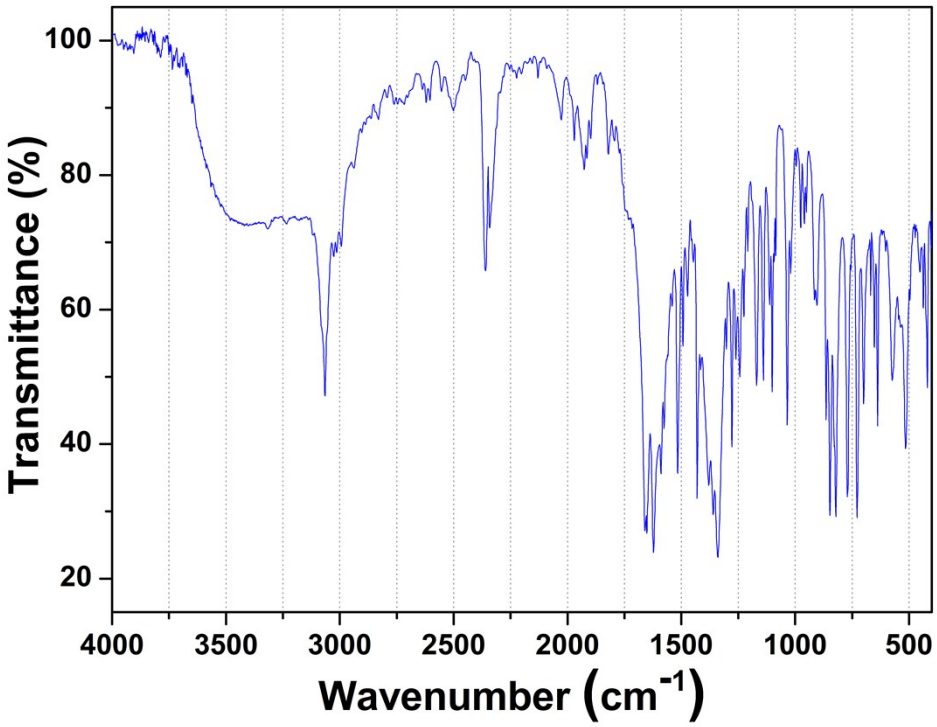

Fig. S2: IR spectrum of $[Cd(C_{12}N_2H_8)(C_7N_1O_4H_3)]$, **1.**

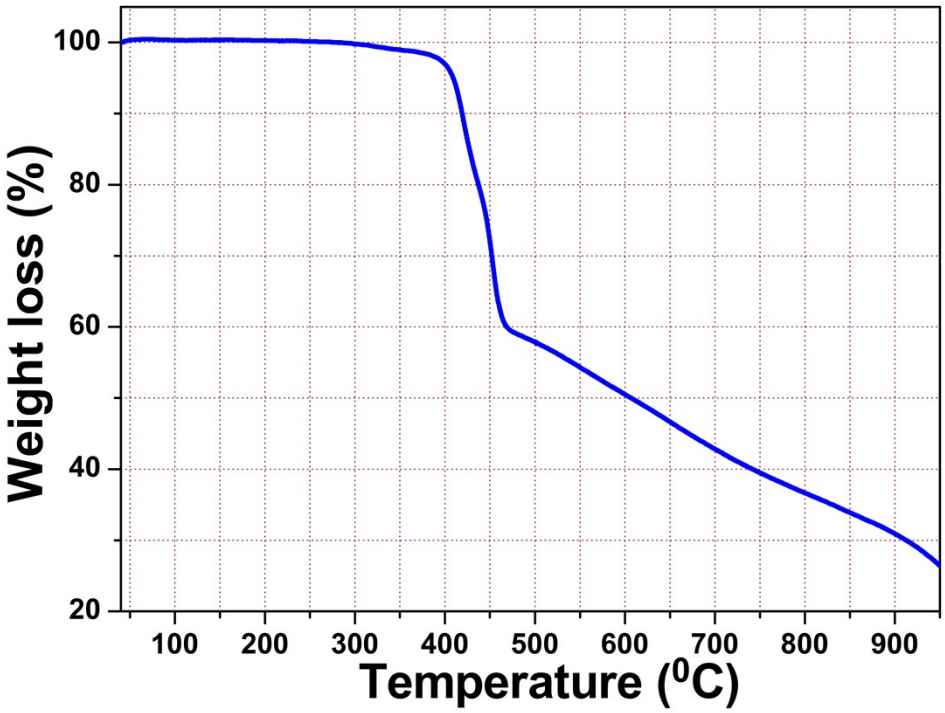

Fig. S3: Thermogravimetric analysis (TGA) of $[Cd(C_{12}N_2H_8)(C_7N_1O_4H_3)]$, **1**, in nitrogen atmosphere.

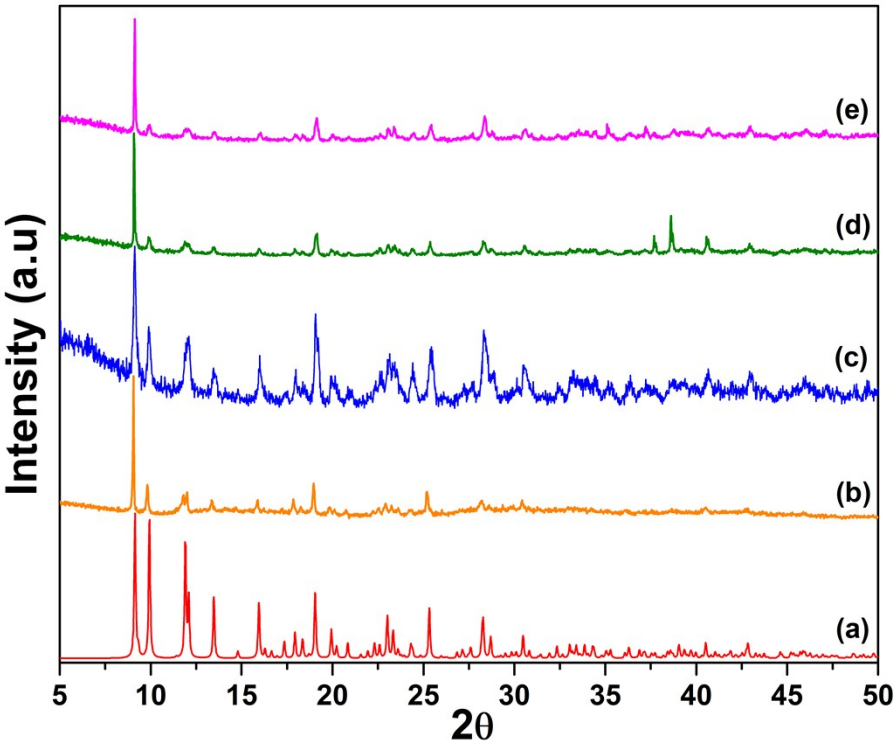

Fig. S4: Powder XRD (CuKα) patterns of $[Cd(C_{12}N_2H_8)(C_7N_1O_4H_3)]$, 1: (a) simulated from single crystal X-ray data, (b) after immersing in water for 2 days, (c) at pH=3 (d) at pH=6 and (e) at pH= 10.

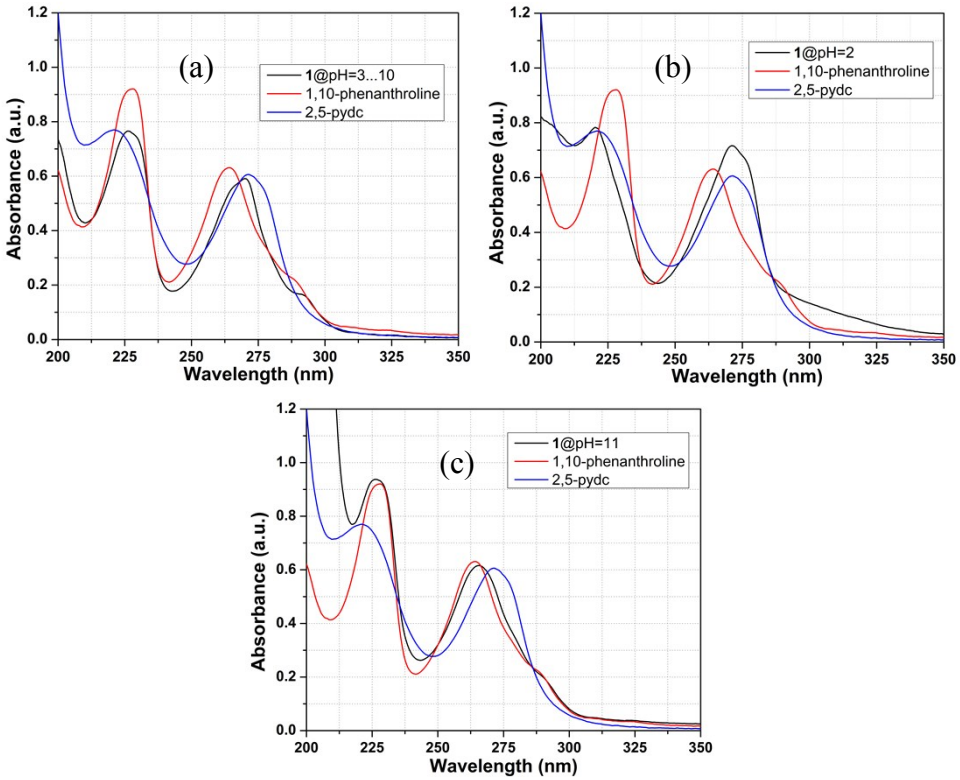

Fig. S5: (a) Absorption spectra of compound **1**, 2,5-pydc and 1,10-phenanthroline in the pH range 3 to 10. It shows the difference in the spectra of compound and the ligands in both peak positions as well as shape of the band. (b) Absorption spectra of compound **1**, 2,5-pydc and 1,10-phenanthroline at pH = 2. In this pH, absorption spectra of compound nicely match (both peak position and the band shape of the spectra) with the absorption spectra of 2,5-pydc (c) Absorption spectra of compound **1**, 2,5-pydc and 1,10-phenanthroline at pH = 11. In this pH, absorption spectra of compound nicely match (both peak position and the band shape of the spectra) with the absorption spectra of 1,10-phenanthroline Both (b) and (c) indicate that the compound in the pH ranges below 3 and above 10 breaks down and the free ligand is formed.

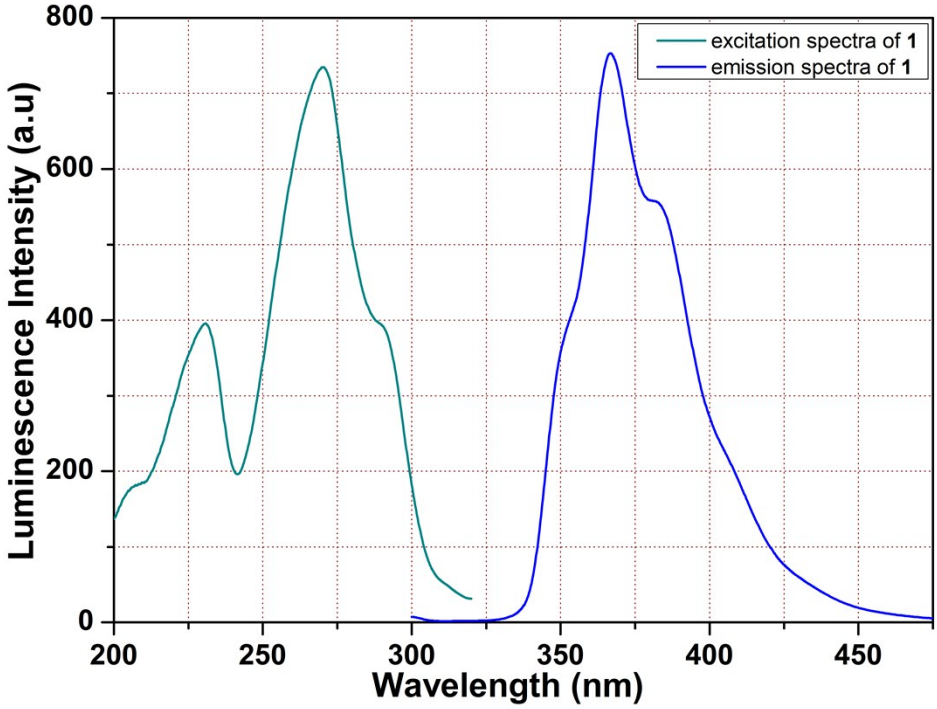

Fig. S6: Excitation and luminescence spectrum (λ_{ex} = 280 nm) of compound **1**.

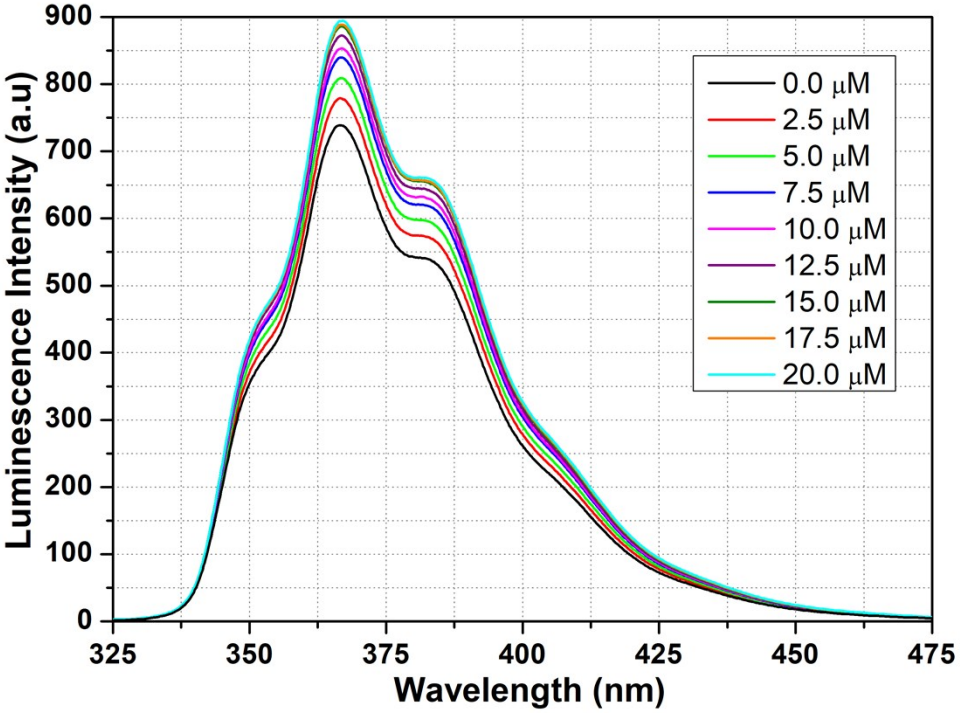

Fig. S7: Emission spectra of compound **1** dispersed in water upon incremental addition of Al^{3+} solution (λ_{ex} = 280 nm). Final concentration of Al^{3+} in the medium is indicated in the legend.

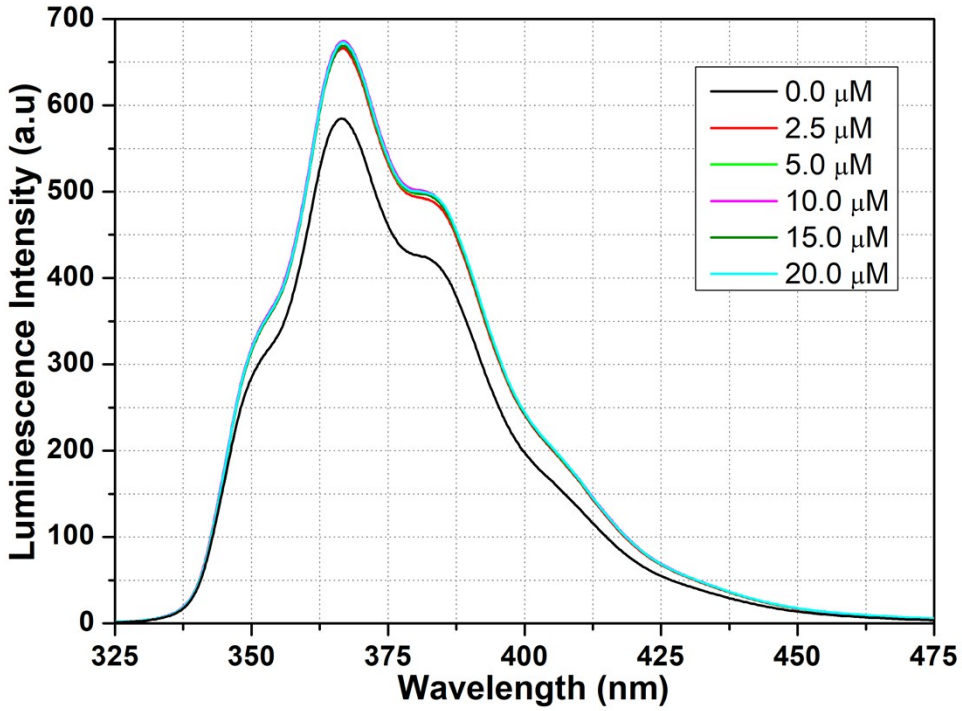

Fig. S8: Emission spectra of compound **1** dispersed in water upon incremental addition of Pb^{2+} solution (λ_{ex} = 280 nm). Final concentration of Pb^{2+} in the medium is indicated in the legend.

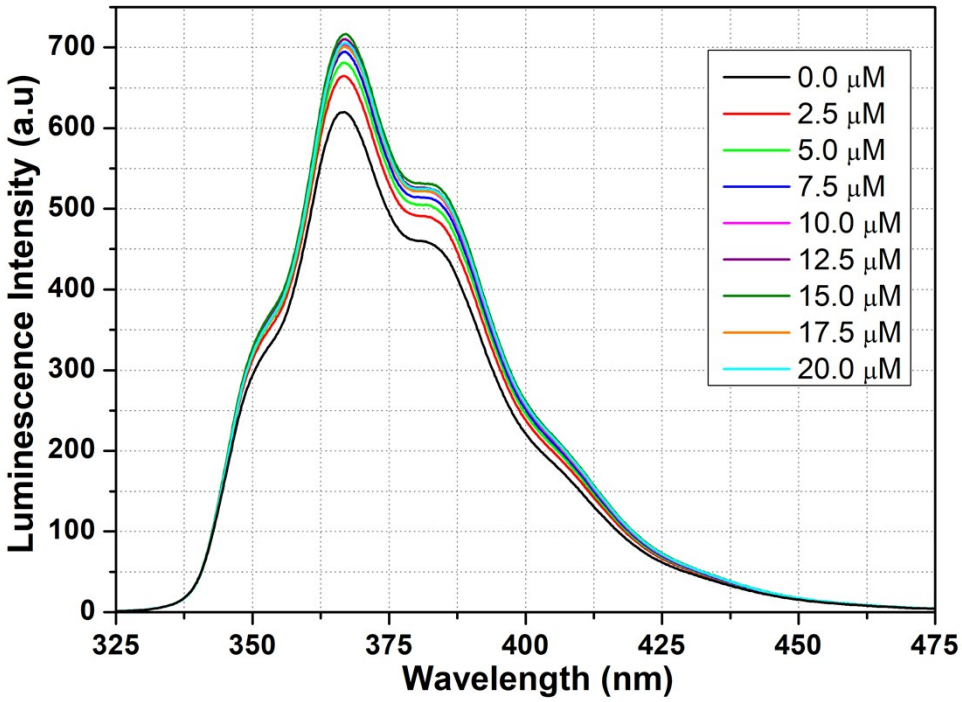

Fig. S9: Emission spectra of compound **1** dispersed in water upon incremental addition of Cd^{2+} solution (λ_{ex} = 280 nm). Final concentration of Cd^{2+} in the medium is indicated in the legend.

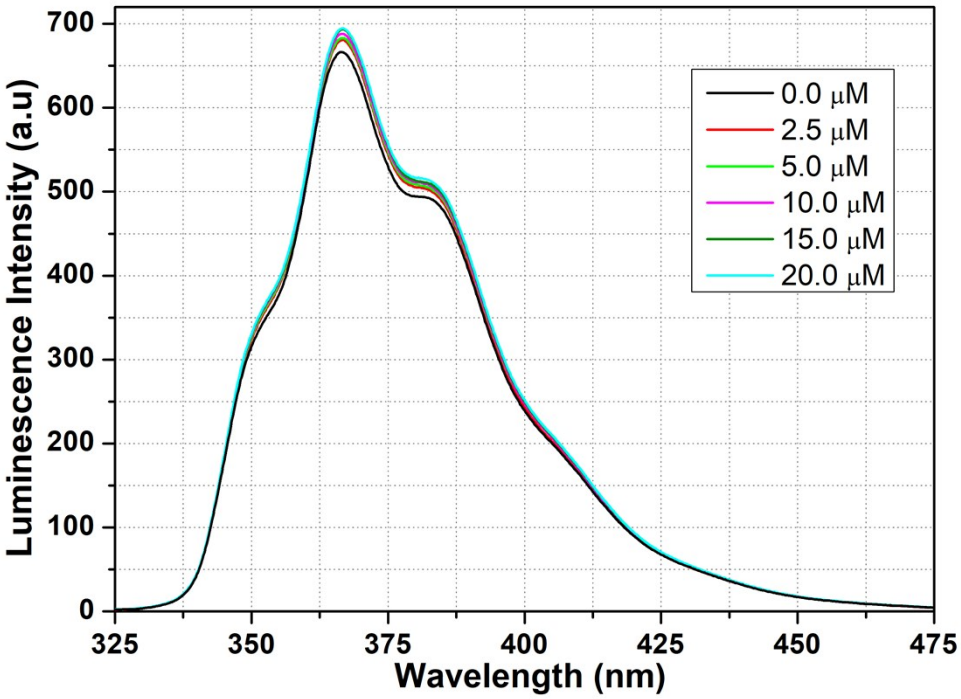

Fig. S10: Emission spectra of compound **1** dispersed in water upon incremental addition of K^+ solution (λ_{ex} = 280 nm). Final concentration of K^+ in the medium is indicated in the legend.

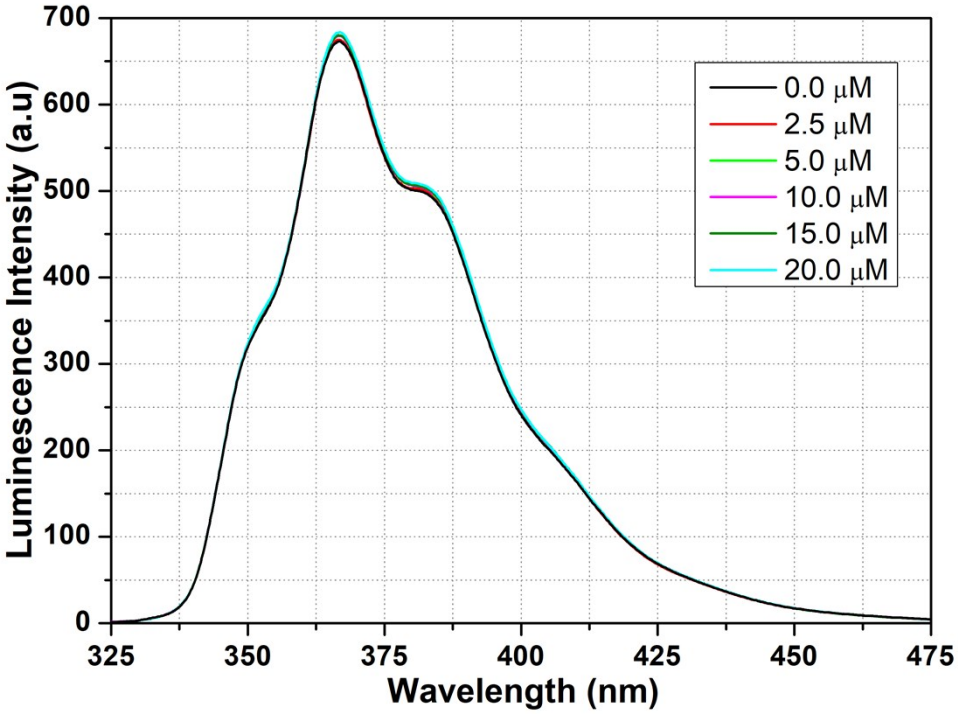

Fig. S11: Emission spectra of compound **1** dispersed in water upon incremental addition of Mg^{2+} solution (λ_{ex} = 280 nm). Final concentration of Mg^{2+} in the medium is indicated in the legend.

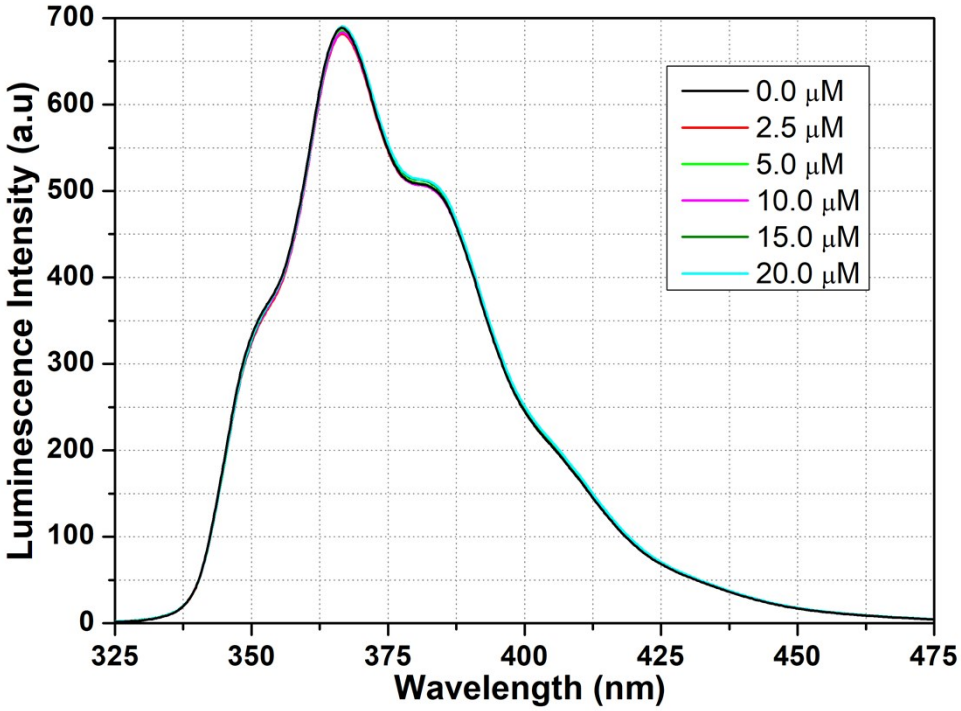

Fig. S12: Emission spectra of compound **1** dispersed in water upon incremental addition of Na^+ solution (λ_{ex} = 280 nm). Final concentration of Na^+ in the medium is indicated in the legend.

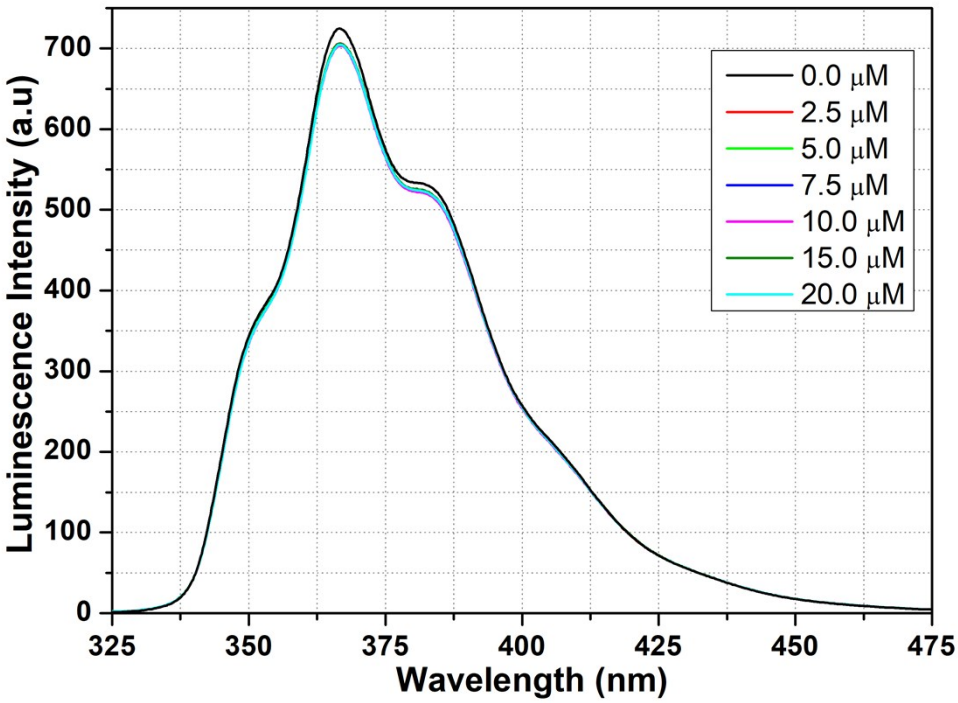

Fig. S13: Emission spectra of compound **1** dispersed in water upon incremental addition of Mn^{2+} solution (λ_{ex} = 280 nm). Final concentration of Mn^{2+} in the medium is indicated in the legend.

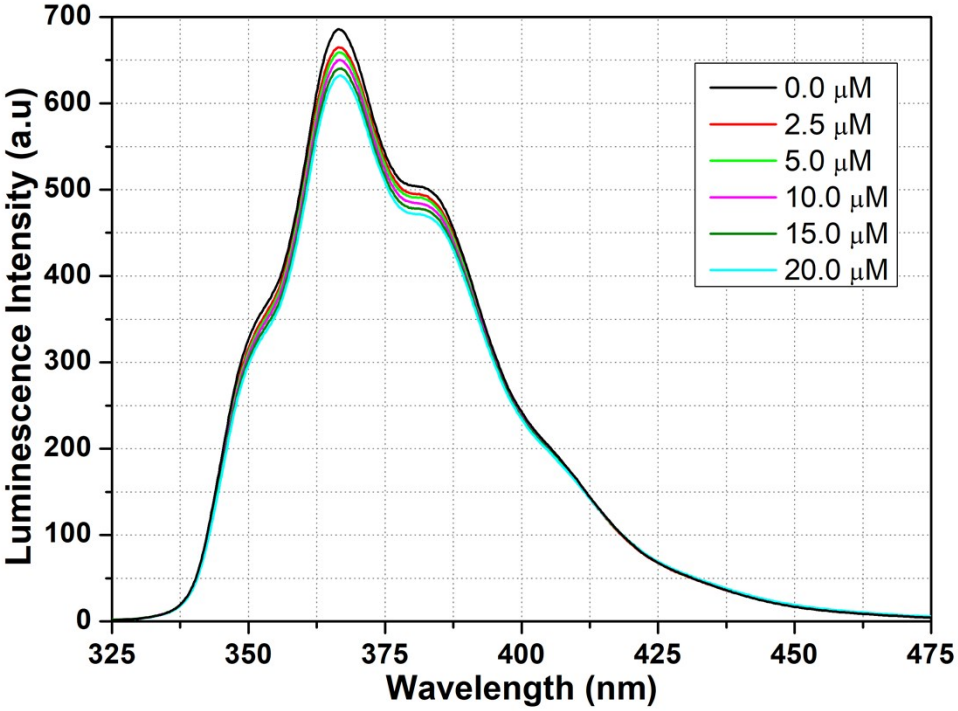

Fig. S14: Emission spectra of compound **1** dispersed in water upon incremental addition of Cr^{3+} solution (λ_{ex} = 280 nm). Final concentration of Cr^{3+} in the medium is indicated in the legend.

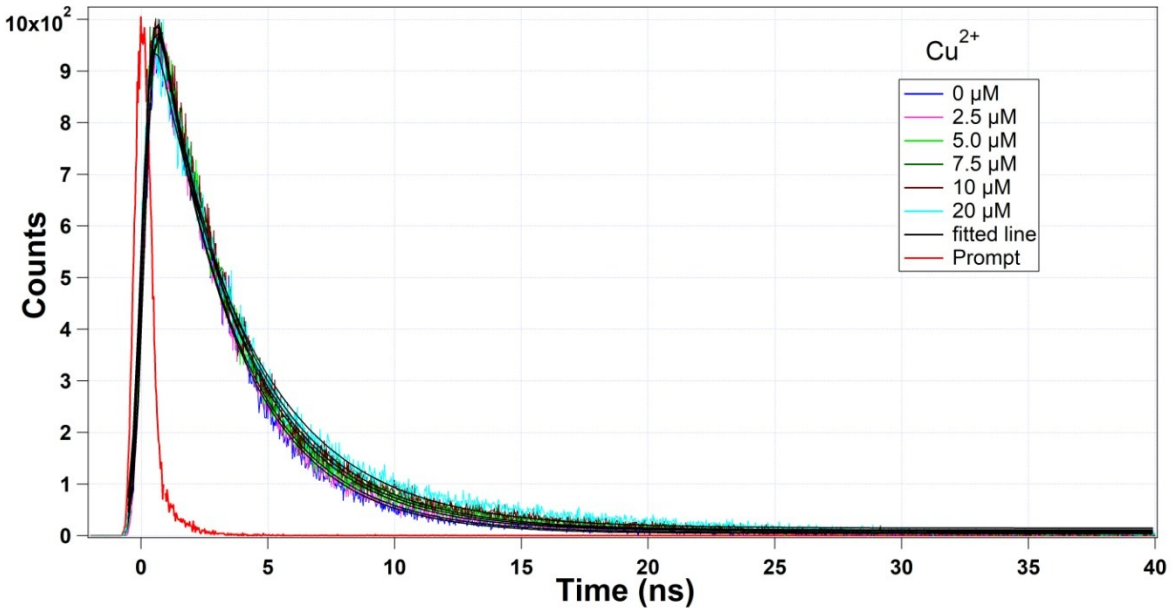

Fig. S15: Time resolved fluorescence decay plot of compound **1** and with addition of Cu^{2+}. Final concentrations of metal ions in the medium are indicated in the legend.

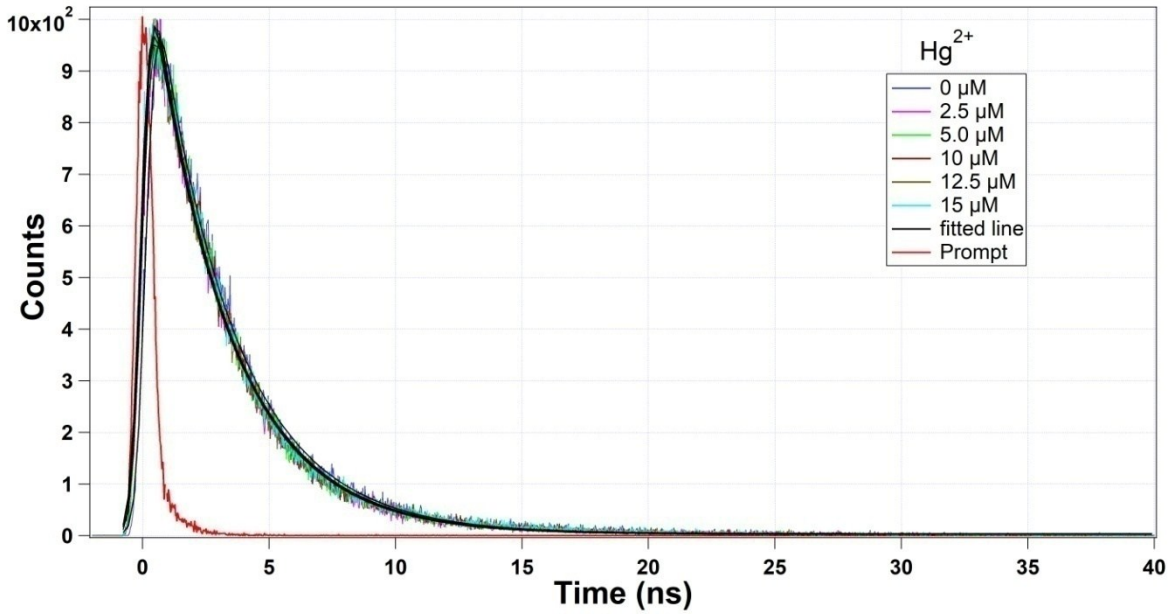

Fig. S16: Time resolved fluorescence decay plot of compound **1** and with addition of Hg^{2+}. Final concentrations of metal ions in the medium are indicated in the legend.

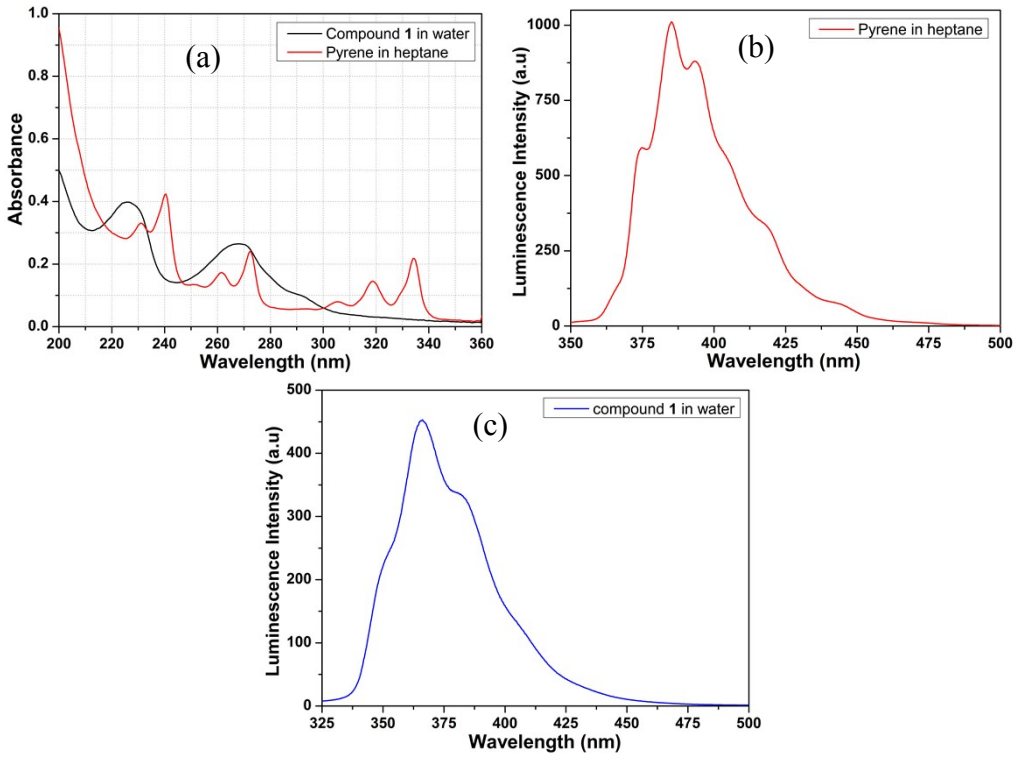

Fig. S17: (a) Absorption spectra of compound **1** in water and pyrene in heptane (b) luminescence spectra of pyrene in heptanes upon excitation at 335 nm (c) luminescence spectra of compound **1** in water upon excitation at 272 nm.

Determination of quantum yield:

$$Q_f^i = \frac{F^i f_s n_i^2}{F^s f_i n_s^2} Q_f^s$$

where Q_f^i and Q_f^s are the fluorescence QYs of the sample and that of the standard, respectively; F^i and F^s are the integrated intensities (areas) of sample and standard spectra, respectively; $f_s and\ f_i$ are the absorbance factor of standard and sample, respectively; the refractive indices of the sample and reference solution are n_i and n_s, respectively.

$$Q_f^i = \frac{20601 \times 0.21 \times 1.33^2}{37475 \times\ 0.24 \times 1.38^2} \times\ 0.3$$

$$Q_f^i =\ 0.13$$

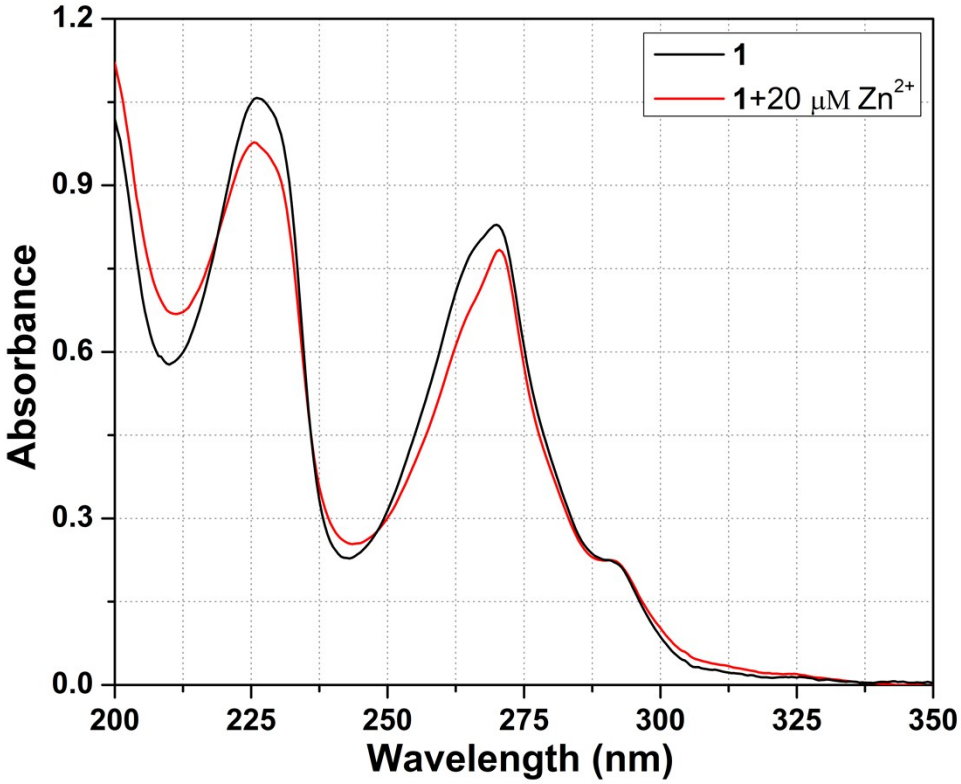

Fig. S18: Absorption spectra of compound **1** and compound **1** + 20 μM Zn^{2+} in aqueous solution. It is also be noted that with the coordination of Zn^{2+} ion, the absorption bands at 270 nm changes its shape which is the clear indication of increase in rigidity of the structure.

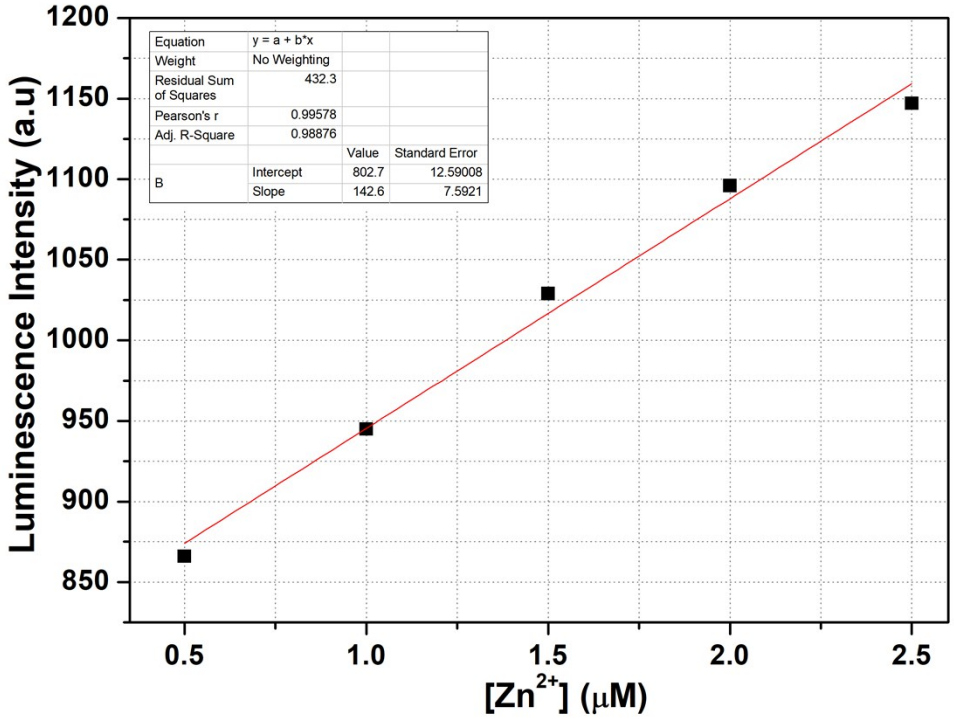

Fig. S19: Linear region of luminescence intensity (at 365 nm) of compound **1** upon addition of Zn^{2+} (R^2 = 0.98876).

Calculation of Detection Limit

Standard deviation for **1**

Blank Reading (only **1**)	Fluorescence Intensity
Reading 1	735
Reading 2	744
Reading 3	755
Reading 4	767
Reading 5	776
Standard deviation(σ)	14.59

Standard Deviation (σ)	14.59
Slope from Graph (m)	142.6 μM^{-1}

Thus, Limit of Detection (LOD) = $3\sigma/m$ = (3×14.59)/142.6 = 0.30 μM = 19 ppb

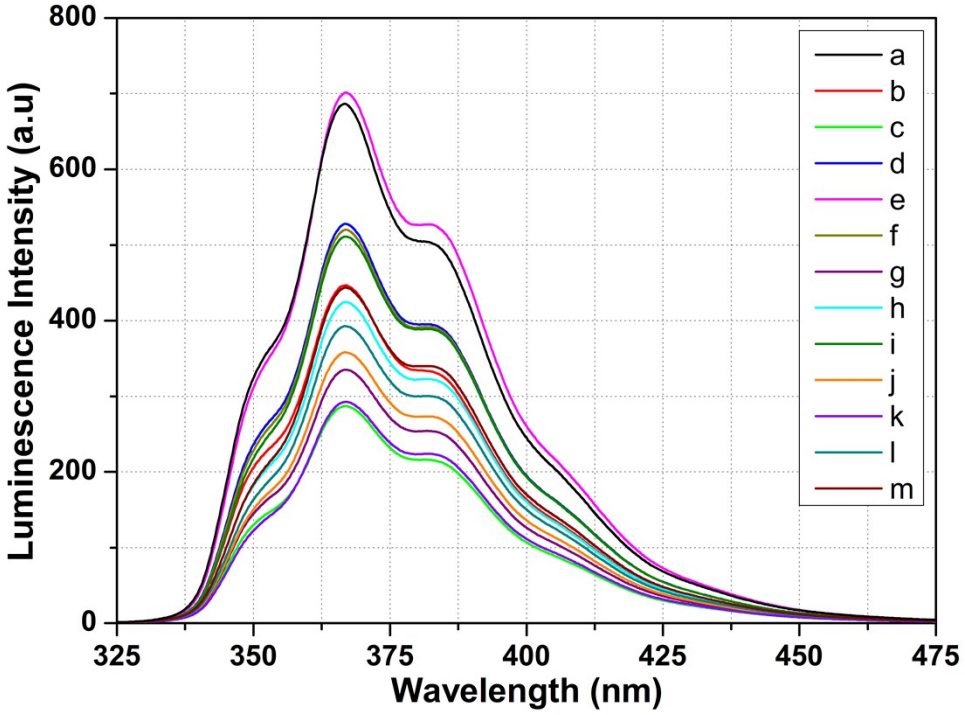

Fig. S20: Emission spectra of the compound **1** dispersed in water upon addition of 5 μM solution of Co^{2+} sequentially in two equal portion (2.5 μM in each portion) followed by 5 μM solution of Zn^{2+} in similar way (λ_{ex} = 280 nm). The addition cycles were repeated for two more times. The final concentration of analytes solution (Co^{2+} and Zn^{2+}) are as below: (a) 0 μM Co^{2+} + 0 μM Zn^{2+}, (b) 2.5 μM Co^{2+} + 0 μM Zn^{2+}, (c) 5 μM Co^{2+} + 0 μM Zn^{2+}, (d) 5 μM Co^{2+} + 2.5 μM Zn^{2+}, (e) 5 μM Co^{2+} + 5 μM Zn^{2+}, (f) 7.5 μM Co^{2+} + 5 μM Zn^{2+}, (g) 10 μM Co^{2+} + 5 μM Zn^{2+}, (h) 10 μM Co^{2+} + 7.5 μM Zn^{2+}, (i) 10 μM Co^{2+} + 10 μM Zn^{2+}, (j) 12.5 μM Co^{2+} + 10 μM Zn^{2+}, (k) 15 μM Co^{2+} + 10 μM Zn^{2+}, (l) 15 μM Co^{2+} + 12.5 μM Zn^{2+}, (m) 15 μM Co^{2+} + 15 μM Zn^{2+}.

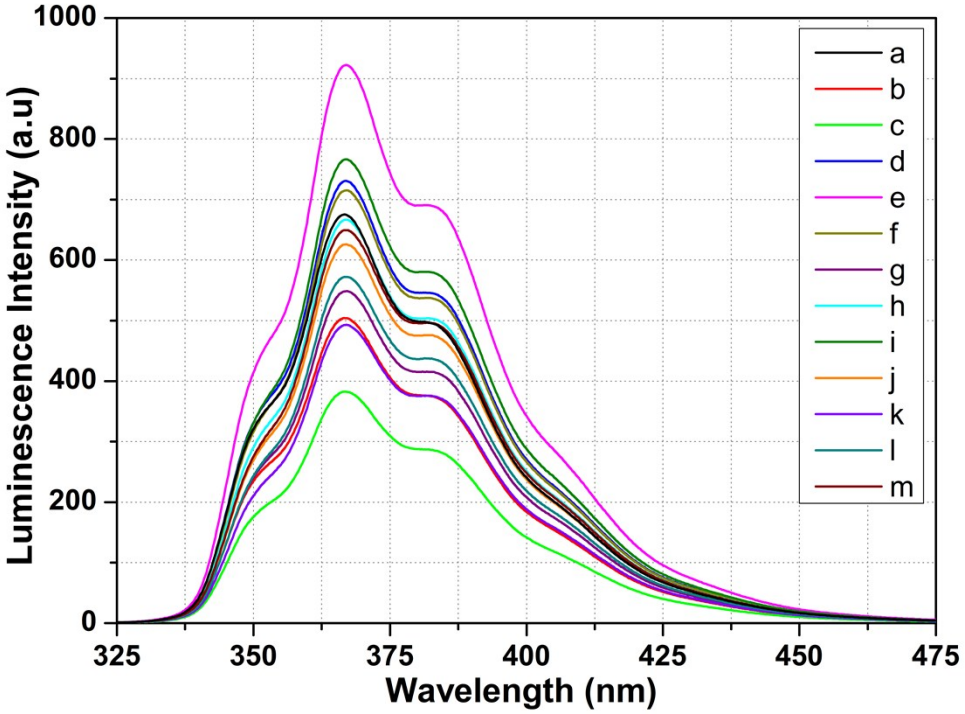

Fig. S21: Emission spectra of the compound **1** dispersed in water upon addition of 5 μM solution of Hg^{2+} sequentially in two equal portion (2.5 μM in each portion) followed by 5 μM solution of Zn^{2+} in similar way (λ_{ex} = 280 nm). The addition cycles were repeated for two more times. The final concentration of analytes solution (Hg^{2+} and Zn^{2+}) are as below: (a) 0 μM Hg^{2+} + 0 μM Zn^{2+}, (b) 2.5 μM Hg^{2+} + 0 μM Zn^{2+}, (c) 5 μM Hg^{2+} + 0 μM Zn^{2+}, (d) 5 μM Hg^{2+} + 2.5 μM Zn^{2+}, (e) 5 μM Hg^{2+} + 5 μM Zn^{2+}, (f) 7.5 μM Hg^{2+} + 5 μM Zn^{2+}, (g) 10 μM Hg^{2+} + 5 μM Zn^{2+}, (h) 10 μM Hg^{2+} + 7.5 μM Zn^{2+}, (i) 10 μM Hg^{2+} + 10 μM Zn^{2+}, (j) 12.5 μM Hg^{2+} + 10 μM Zn^{2+}, (k) 15 μM Hg^{2+} + 10 μM Zn^{2+}, (l) 15 μM Hg^{2+} + 12.5 μM Zn^{2+}, (m) 15 μM Hg^{2+} + 15 μM Zn^{2+}.

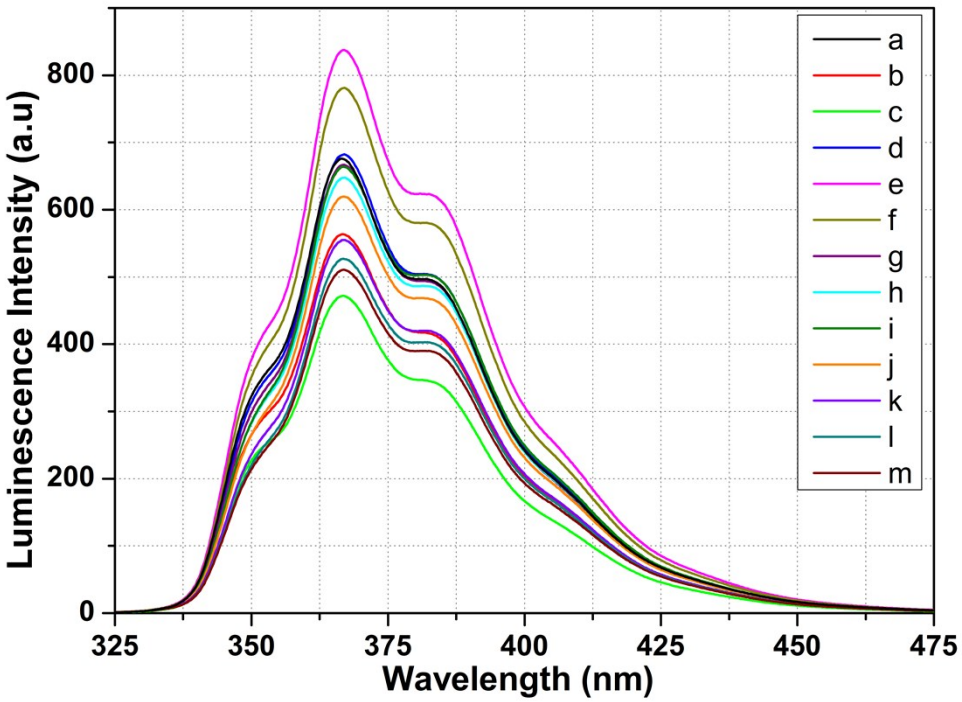

Fig. S22: Emission spectra of the compound **1** dispersed in water upon addition of 5 μM solution of Ni^{2+} sequentially in two equal portion (2.5 μM in each portion) followed by 5 μM solution of Zn^{2+} in similar way (λ_{ex} = 280 nm). The addition cycles were repeated for two more times. The final concentration of analytes solution (Ni^{2+} and Zn^{2+}) are as below: (a) 0 μM Ni^{2+} + 0 μM Zn^{2+}, (b) 2.5 μM Ni^{2+} + 0 μM Zn^{2+}, (c) 5 μM Ni^{2+} + 0 μM Zn^{2+}, (d) 5 μM Ni^{2+} + 2.5 μM Zn^{2+}, (e) 5 μM Ni^{2+} + 5 μM Zn^{2+}, (f) 7.5 μM Ni^{2+} + 5 μM Zn^{2+}, (g) 10 μM Ni^{2+} + 5 μM Zn^{2+}, (h) 10 μM Ni^{2+} + 7.5 μM Zn^{2+}, (i) 10 μM Ni^{2+} + 10 μM Zn^{2+}, (j) 12.5 μM Ni^{2+} + 10 μM Zn^{2+}, (k) 15 μM Ni^{2+} + 10 μM Zn^{2+}, (l) 15 μM Ni^{2+} + 12.5 μM Zn^{2+}, (m) 15 μM Ni^{2+} + 15 μM Zn^{2+}.

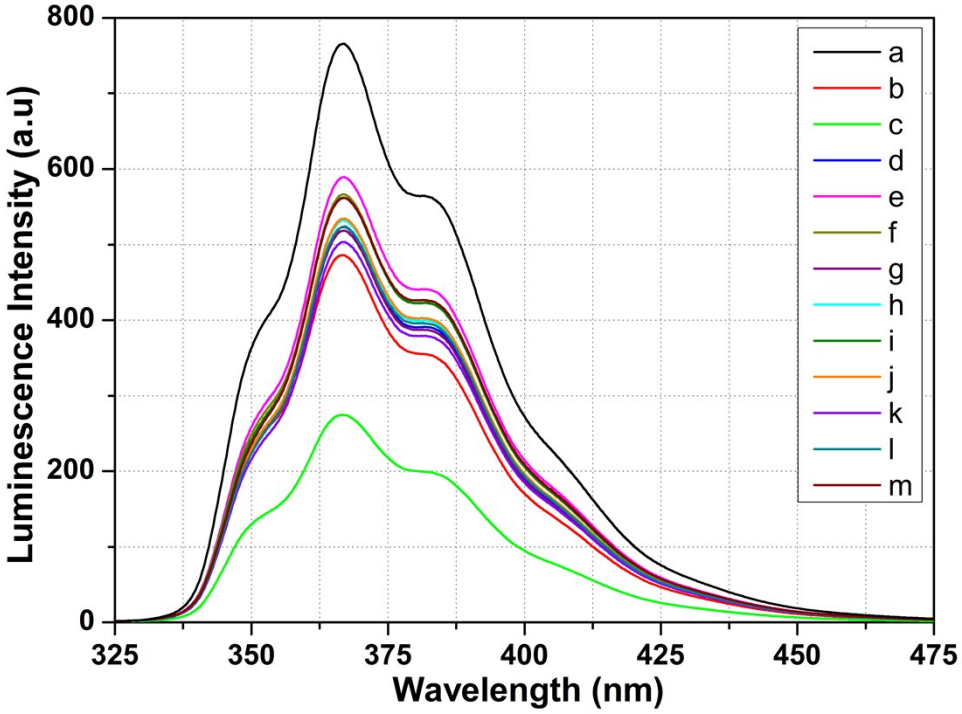

Fig. S23: Emission spectra of the compound **1** dispersed in water upon addition of 5 μM solution of Fe^{2+} sequentially in two equal portion (2.5 μM in each portion) followed by 5 μM solution of Zn^{2+} in similar way (λ_{ex} = 280 nm). The addition cycles were repeated for two more times. The final concentration of analytes solution (Fe^{2+} and Zn^{2+}) are as below: (a) 0 μM Fe^{2+} + 0 μM Zn^{2+}, (b) 2.5 μM Fe^{2+} + 0 μM Zn^{2+}, (c) 5 μM Fe^{2+} + 0 μM Zn^{2+}, (d) 5 μM Fe^{2+} + 2.5 μM Zn^{2+}, (e) 5 μM Fe^{2+} + 5 μM Zn^{2+}, (f) 7.5 μM Fe^{2+} + 5 μM Zn^{2+}, (g) 10 μM Fe^{2+} + 5 μM Zn^{2+}, (h) 10 μM Fe^{2+} + 7.5 μM Zn^{2+}, (i) 10 μM Fe^{2+} + 10 μM Zn^{2+}, (j) 12.5 μM Fe^{2+} + 10 μM Zn^{2+}, (k) 15 μM Fe^{2+} + 10 μM Zn^{2+}, (l) 15 μM Fe^{2+} + 12.5 μM Zn^{2+}, (m) 15 μM Fe^{2+} + 15 μM Zn^{2+}.

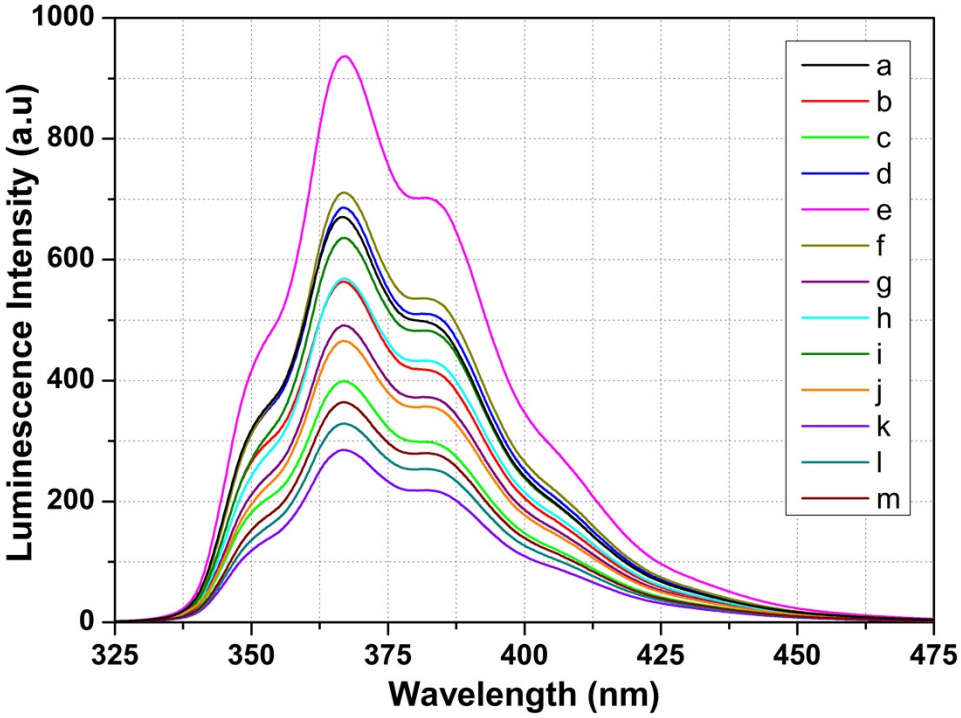

Fig. S24: Emission spectra of the compound **1** dispersed in water upon addition of 5 μM solution of Cu^{2+} sequentially in two equal portion (2.5 μM in each portion) followed by 5 μM solution of Zn^{2+} in similar way (λ_{ex} = 280 nm). The addition cycles were repeated for two more times. The final concentration of analytes solution (Cu^{2+} and Zn^{2+}) are as below: (a) 0 μM Cu^{2+} + 0 μM Zn^{2+}, (b) 2.5 μM Cu^{2+} + 0 μM Zn^{2+}, (c) 5 μM Cu^{2+} + 0 μM Zn^{2+}, (d) 5 μM Cu^{2+} + 2.5 μM Zn^{2+}, (e) 5 μM Cu^{2+} + 5 μM Zn^{2+}, (f) 7.5 μM Cu^{2+} + 5 μM Zn^{2+}, (g) 10 μM Cu^{2+} + 5 μM Zn^{2+}, (h) 10 μM Cu^{2+} + 7.5 μM Zn^{2+}, (i) 10 μM Cu^{2+} + 10 μM Zn^{2+}, (j) 12.5 μM Cu^{2+} + 10 μM Zn^{2+}, (k) 15 μM Cu^{2+} + 10 μM Zn^{2+}, (l) 15 μM Cu^{2+} + 12.5 μM Zn^{2+}, (m) 15 μM Cu^{2+} + 15 μM Zn^{2+}.

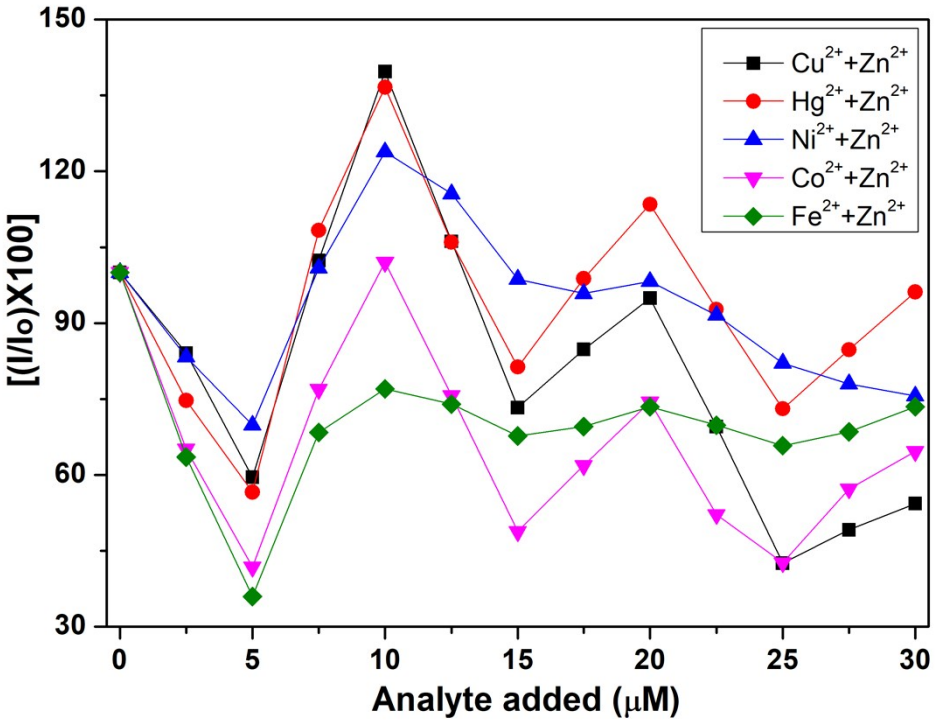

Fig. S25: : Change of percentage in luminescence intensity upon the addition of quenchable metal ions (two steps, 2.5 μM + 2.5 μM) followed by the addition of Zn^{2+} solution (two steps, 2.5 μM + 2.5 μM) and so on.

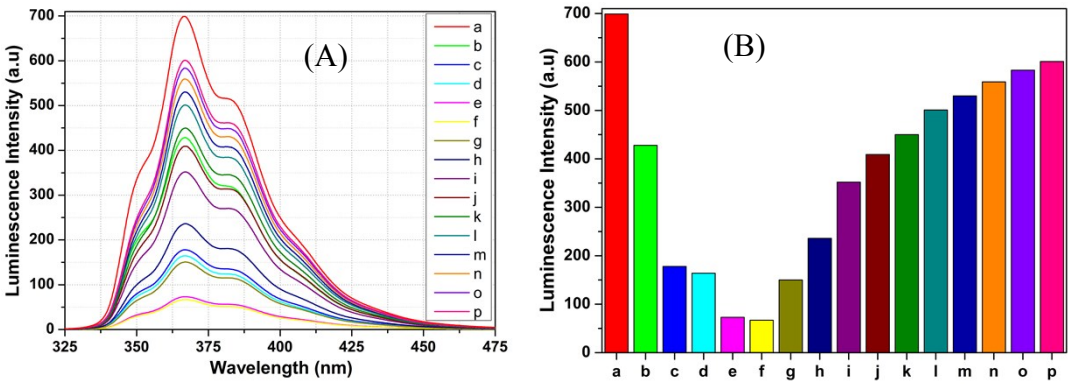

Fig. S26: (A) Emission spectra of **1** in aqueous solution upon the incremental addition of Zn^{2+} solution in presence of 5 μM of quenchable metal ions solution (λ_{ex} = 280 nm). (B) Bar diagram showing the luminescence intensity (monitored at 365 nm) of **1** upon the incremental addition of Zn^{2+} solution in presence of 5 μM of each quenchable metal ions solution. The composition and concentration of the system were as follows: (a) **1** in aqueous solution, (b) a + 5 μM Cu^{2+}, (c) b + 5 μM Hg^{2+}, (d) c + 5 μM Ni^{2+}, (e) d + 5 μM Co^{2+}, (f) e + 5 μM Fe^{2+}, (g) f + 2.5 μM Zn^{2+}, (h) g + 5 μM Zn^{2+}, (i) g + 7.5 μM Zn^{2+}, (j) g + 10 μM Zn^{2+}, (k) g + 12.5 μM Zn^{2+}, (l) g + 15 μM Zn^{2+}, (m) g + 17.5 μM Zn^{2+}, (n) g + 20 μM Zn^{2+} , (o) g +22.5μM Zn^{2+} and (p) g +25μM Zn^{2+}.